journal

J. Am. Ceram. Soc., 92 [12] 3044–3051 (2009)
DOI: 10.1111/j.1551-2916.2009.03327.x

Effect of Segregating Impurities on the Grain-Boundary Character Distribution of Magnesium Oxide

Francine Papillon, Gregory S. Rohrer, and Paul Wynblatt†

Department of Materials Science and Engineering, Carnegie Mellon University, Pittsburgh, PA 15213

The grain-boundary character distribution (GBCD) of undoped MgO has been measured and compared with samples containing small concentrations of Ca, Sr, Ba, and Y. Auger electron spectroscopy measurements of intergranular fracture surfaces verified that Ca, Ba, and Y segregated anisotropically to grain boundaries (GBs). The segregation of Sr was not detected. The GBCDs of Ca, Ba, and Y doped MgO have more GBs comprised of {100} planes than the undoped material and the fractional area of these planes was highest in the Ca-containing samples. Sr impurities, on the other hand, have no measurable influence on the GBCD. The results demonstrate that GB plane distributions can be controlled through impurity additions.

I. Introduction

Solute segregation to grain boundaries (GBs) is a well-established phenomenon that refers to a localized increase in concentration of one or several components at interfaces, and which is driven by the decrease in interfacial free energy that accompanies the adsorption process.[1] The anisotropy of the GB energy is also thought to be linked to the types of GBs that occur within polycrystals.[2] The distribution of GB types is quantified by the grain-boundary character distribution (GBCD), which is a measure of the relative areas of different types of GBs, distinguished by their lattice misorientations and GB plane orientations. Because the GBCD is determined by relative GB energies, and because segregation will alter the anisotropy of these energies, it should be possible to influence the types of GBs that occur in a polycrystal through the addition of impurities.[3–8]

The purpose of this work is to determine how selected impurities affect the GBCD of MgO. This was accomplished by measuring the GBCDs of "pure" (not intentionally doped) MgO, and of MgO containing selected impurities, using a stereological analysis of electron backscatter diffraction (EBSD) maps.[2] Ca, Sr, Ba, and Y were selected for study because they are either known or expected to segregate to MgO GBs.[8,9] One of the major contributions to the driving force of segregation in MgO is the solute strain energy which results from the size misfit between the ions of the solute and the solvent[10] (see Table I [11,12]). In addition, electrostatic effects, due to the interaction of aliovalent impurity cations with the space charge associated with GBs, are expected to play a role in the case of Y segregation to GBs in MgO. Auger electron spectroscopy (AES) of intergranular fracture surfaces was used to quantify the degree of segregation.

The five parameter GBCD of a MgO sample with a small but significant (0.2%) concentration of Ca has been reported previously.[13] The prior work revealed a significant texture in the distribution of GB planes. In particular, it was shown that for GBs of low misorientation angles, there is a preference for tilt boundaries, especially those with plane normals in the ⟨110⟩ direction. At all fixed misorientations >10°, there was also a preference for boundaries with ⟨100⟩ boundary plane normals. This preference is substantial because the {100} planes occur twice as frequently as other types of GBs.

As already shown in various studies of crystalline materials,[3–5] the degree of solute segregation differs among GBs of different character. In their work on surface segregation, Tasker *et al.*[9] showed that Ca^{2+}, Sr^{2+}, and Ba^{2+} will segregate to the (100) surface of MgO. Some recent results have shown that there is a strong correlation between Nb segregation and GB plane orientation in Nb-doped TiO_2,[6] and that Nb-doping of TiO_2 modifies the frequency with which certain GB planes are observed.[7] Also, as described in a previous paper,[8] preliminary results on Ca-doped MgO showed the existence of a strong anisotropy of GB segregation, with a variation of up to a factor of six between low and high segregation GBs. Thus, there are ample grounds to suppose that doping MgO with GB-segregating impurities will have an effect on the GBCD.

II. Experimental Procedure

(1) Sample Preparation

A reference sample of undoped MgO and five MgO specimens doped with Ca, Sr, Ba, and Y were prepared for this study. The nominal compositions of these samples are summarized in Table II. The starting material for the undoped MgO sample was a carbonate powder of 99.996% purity. High purity dopant powders were used to reduce possible interference from uncontrolled impurities. The Ca, Sr, and Ba, doped samples were prepared by mixing carbonate powders and calcining in air at 1100°C for 15 h. The calcined powder was re-ground and compacted in a uniaxial press, and the resulting pellets were sintered at 1600°C for 15 h. The calcination was carried out in magnesia crucibles (Ozark, Webb City, MO, MgO 99.38%). During sintering, the pellets were embedded in pure MgO powder within three nested magnesia crucibles. Finally, the samples were polished and thermally etched in air at 1400°C for 2–5 h to reveal the GBs. The Y-doped samples were treated in exactly the same way as the others, but yttrium oxide was used as the source instead of the carbonate. The grain sizes are reported in Table II.

Dopants were added in nominal quantities that may have exceeded the solubility limits, as these are not known for most of the doping elements. ICP analysis was performed on the samples, but gave irreproducible results. Thus, the quantitative data obtained is not considered reliable. With the exception of the Ba-doped samples, the results confirmed the presence of the added impurities, but at lower concentrations than the nominal compositions. While the ICP did not detect Ba in the Ba-doped sample, this dopant was detected on the GB fractures by AES (as described in more detail in subsequent sections), so there is no question of its presence in that sample. Therefore, while we cannot be certain of the bulk compositions, we can be certain that the samples contained the added impurities.

H. Chan—contributing editor

Manuscript No. 25988. Received March 10, 2009; approved July 7, 2009.
This work was supported by the MRSEC Program of the National Science Foundation under Award No. DMR-0520425.
†Author to whom correpsondence should be addressed. e-mail: pw01@andrew.cmu.edu

Table I. Octahedral Ionic Crystal Radii[4]

Element	Ionic radius (10^{-10} m)
Mg^{2+}	0.72
Ca^{2+}	1.00
Ba^{2+}	1.35
Sr^{2+}	1.18
Y^{3+}	0.90

(2) GB Character and Stereological Analysis

A GB's crystallographic characteristics are specified by five macroscopic parameters. Three Euler angles (φ_1,Φ, φ_2) can be used to specify the transformation that brings one crystal into coincidence with another and, therefore, define the lattice misorientation (Δg). Two spherical angles (θ and ϕ) can be used to specify the orientation of the GB plane normal (n) in the crystal reference frame. The relative areas of different types of interfaces, distinguished by Δg and n, were determined using a previously described stereological technique.[14] The observations needed for the stereological analysis are line segments approximating GB traces, in the sample reference frame, and the orientations of the crystals adjacent to each segment. These segments were extracted from the orientation maps using the orientation imaging microscopy (OIM) software.[15]

From these data, several related quantities can be derived. The GB normal distribution in the crystal reference frame, $\lambda(n)$, depends on only two spherical angles and has the symmetry of the crystal. The GB normal distribution in the bicrystal reference frame, $\lambda(\Delta g,n)$, differs for each value of the misorientation and has the symmetry of the bicrystal. These distributions are plotted on stereographic projections in units of multiples of a random distribution (MRD), where unity corresponds to the population that is expected in a random distribution.

(3) Orientation Data Acquisition

Crystal orientation maps were obtained on planar sections by OIM, within a scanning electron microscope (SEM Philips XL40 FEG, Eindhoven, the Netherlands). The computer-assisted TSL OIM system (TexSEM Laboratories, Provo, UT) automatically indexes EBSD patterns, which specify the local orientation of the crystal at each position where the beam is diffracted. In this work, the samples were positioned at a 60° tilt angle with respect to the direction of the incident beam. Multiple areas of 1 mm^2 or less were mapped on the surface of each specimen and grain orientations was recorded every 2 μm on a square coordinate grid. In the case of the Y-doped sample, a 6 μm step size was chosen due to its larger grain size (see Table II). With the exception of the Sr-doped sample, there were at least 10 orientation points per average grain diameter, which is considered sufficient for an accurate determination of the GB positions and, hence, the GBCD. The anisotropy of the Sr-doped sample may be underestimated because there were only five orientation points per grain diameter. To eliminate charging effect in the vacuum chamber of the microscope, a thin carbon coating was applied to all of the samples.

Table II. MgO and Doped MgO Samples Characteristics

Sample	Nominal solute concentration (wt%)	Powder purity	Average grain size (μm)
"Pure" MgO	—	Mg CO_3 99.996%	24
Ca-doped MgO	0.1% Ca	Ca CO_3 99.999%	34
	0.3% Ca		24
Ba-doped MgO	0.1% Ba	Ba CO_3 99.997%	28
Sr-doped MgO	0.1% Sr	Sr CO_3 99.994%	10
Y-doped MgO	0.1% Y	Y_2O_3 99.99%	73

The EBSD maps were processed using a grain dilation clean-up in the TSL OIM software to remove spurious observations. In this procedure, a minimum grain size (10 pixels) and a maximum disorientation angle among pixels within a single grain (5°) are defined. Pixels not belonging to grains meeting these criteria are then reassigned to neighboring grains meeting these criteria. All of the orientations within a single grain are then averaged to produce a single orientation that is assigned to all of the pixels within a grain. GB traces are extracted using the criteria that the line segment used to approximate the GB position does not differ from the actual position by more than 2 pixels.

The stereological analysis used in this work requires that a minimum number of GBs be characterized to ensure reliability in the resulting values of the functions $\lambda(n)$ and $\lambda(\Delta g,n)$. This minimum number depends on the crystal symmetry of the material and the angular resolution of the function.[13] For cubic crystals, and a resolution of 10°, a minimum of 2×10^3 GBs must be measured for $\lambda(n)$, and 5×10^4 GBs for $\lambda(\Delta g,n)$. The numbers of GBs analyzed for each sample are given in Table III.

(4) GB Segregation Measurements

The chemical composition of GBs was determined by AES performed in a scanning Auger microscope on GB surfaces prepared by intergranular fracture. In general, the fractures obtained were predominantly intergranular, as illustrated in Fig. 1, which displays a secondary electron image from a Ca-doped MgO sample. Cleavage features were also occasionally observed, indicating the presence of some transgranular fracture. These areas were systematically avoided for the purpose of the GB compositional analyses. In this work, both GB surfaces on opposite sides of the facture surface were chemically analyzed for the Ca and Ba-doped samples. To reduce charging, samples were tilted within the chamber of the scanning Auger microscope. Even with this procedure, some of the AES spectra had to be discarded due to distortion by charging effects. The following Auger peaks were used for the analyses: 1174 eV in the case of Mg, 291 eV for Ca, 584 eV for Ba, and 127 eV for Y. In the case of Sr-doped samples, GB compositional analyses were performed, however the Sr Auger peak could not be measured because of its low intensity and of interference from other peaks.

III. Results

(1) Chemical Compositions of Fracture Surfaces

The compositions on both sides of about 100 GBs were determined on fracture surfaces of undoped MgO. No significant contamination by Ca, the most common segregating impurity, was detected (the average Ca/Mg peak ratio was 0.06 ± 0.12). However a significant number of GBs contained some excess Si (Si/Mg peak ratio of 0.16 ± 0.14).

The AES results indicate that Ca, Ba, and Y segregate to MgO GBs in the doped samples. In MgO doped with 0.3% Ca, GB compositions were determined on both sides of about 200 GBs. The results showed significant differences in Ca segregation between the two sides of a given GB, as illustrated in Fig. 2(a) where the Ca/Mg Auger peak ratio is displayed for 20 of those GBs. In addition, the distribution of GB compositions,

Table III. Orientation Imaging Microscopy Acquisition Data

Sample	Total number of analyzed grains	Total number of extracted grain boundaries
Undoped MgO	18 950	60 863[†]
Ca-doped MgO	0.3% Ca 18 360	56 682[†]
	0.1% Ca 1687	5162
Ba-doped MgO	3120	9710
Sr-doped MgO	24 313	75 545[†]
Y-doped MgO	1313	7054

[†]Only these three samples had the required numbers of segments to allow a reliable acquisition of $\lambda(\Delta g,n)$.

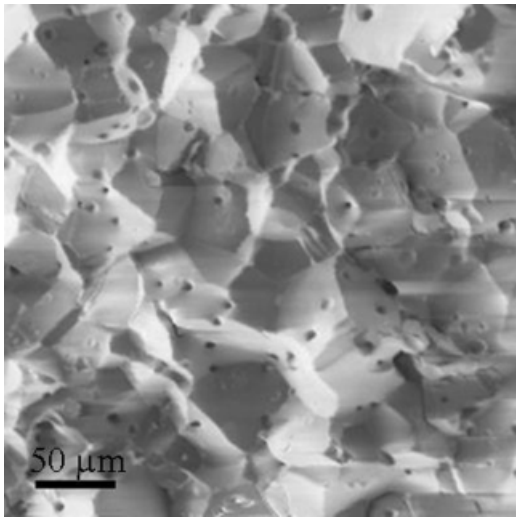

Fig. 1. Secondary electron image of fracture surface of 0.1% Ca-doped MgO obtained in the scanning Auger microscope at an incident electron energy of 3 kV, showing that the fracture surface is predominantly intergranular.

expressed as the fraction of GBs which display a given value of the Ca/Mg Auger peak ratio, is shown in Fig. 2(b). The Ca/Mg Auger peak ratio ranges from ~ 0 to ~ 1, with an average value of 0.38 ± 0.19. Similar results were obtained in measurements on 28 GBs in Ba-doped MgO. These are shown in Figs. 2(c) and (d), and indicate an average value of the Ba/Mg Auger peak ratio of 0.19 ± 0.08. The compositions of 28 GBs in Y-doped MgO had an average Y/Mg Auger peak ratio of 0.20 ± 0.03. However, the Y-doped samples also showed some Ca segregation at the GBs, indicating some Ca-contamination of that sample.

(2) Grain Orientation Distribution

The inverse pole figure (IPF) map presented in Fig. 3 is a typical microstructure obtained for undoped MgO. The orientation distribution functions (ODF) for each of the specimens were calculated using the TSL software. For the most part, the samples were untextured. The largest peak in the inverse pole figures (2.4 MRD) occurred at the [111] position of the Y-doped sample. In the other samples, the peaks did not exceed 1.4 MRD. This weak texture will not bias the stereological procedure.[14] It should be noted that the texture in these samples differs significantly from that of the MgO samples studied by Saylor *et al.*[13] In that earlier study, the processing method created strong $\langle 111 \rangle$ axial texture with a peak of 11 MRD. The misorientation distributions for each sample were also calculated and did not differ significantly from random.

(3) λ(n): GB Normal Distribution in the Crystal Reference Frame

The GB normal distributions in the crystal reference frame, $\lambda(n)$, are presented for all samples in Fig. 4. The distributions are plotted on stereographic projections and the colors represent relative populations in units of MRD. Note that in each case, the range is set by the maximum and minimum of the data. The apparent anisotropy of the undoped MgO and Sr-doped MgO samples, having minima of about 0.9 MRD and maxima of about 1.15 MRD, is relatively weak. Recent work has demonstrated that differences of 10% in the extrema should not be considered significant.[16] The peaks in these distributions are only modestly above the 10% threshold and, therefore,

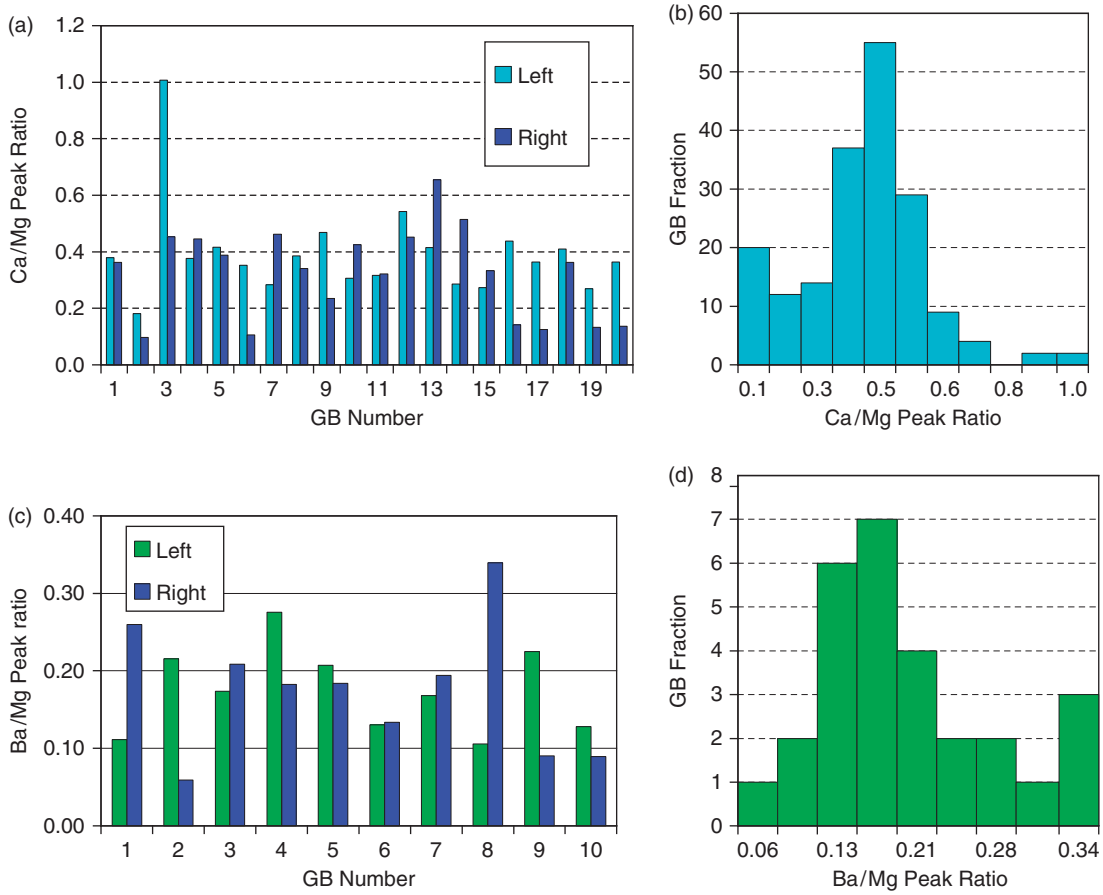

Fig. 2. Ca/Mg and Ba/Mg Auger peak ratios measured on both sides of certain grains on grain boundary (GB) fracture surfaces (a) in 0.3% Ca-doped MgO and (c) in Ba-doped MgO, and distributions of GB segregation over a total of (b) 200 grains in Ca-doped MgO and (d) 28 grains in Ba-doped MgO.

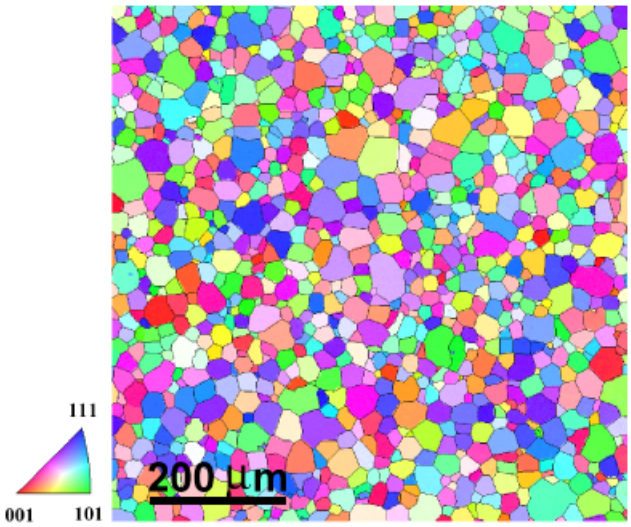

Fig. 3. Inverse pole figure maps obtained on the undoped MgO by orientation imaging microscopy, displaying the orientation of approximately 1500 grains per area after annealing at 1600°C for 15 h. The stereographic triangle provides the color coding for orientations.

have very weak anisotropy. In the Ca, Ba, and Y-doped samples, however, there is more significant anisotropy favoring the {100} orientation. For the Ca-doped samples, there are minima at {111} while for the Sr, Ba, and Y-doped MgO, the minima are at {110}. For the two Ca-doped samples, {100} GB plane orientations are observed more than twice as frequently as expected in a random distribution (2.14 MRD for 0.1% Ca and 2.06 MRD for 0.3%). The differences between these distributions are considered insignificant and, therefore, the samples are equivalent. Interestingly, these distributions are also indistinguishable from the previous work.[13]

(4) λ(Δg,n): GB Normal Distributions in the Bicrystal Reference Frame

The GB plane distributions for misorientations about the [100], [110] and [111] axes for the undoped and 0.3% Ca-doped MgO are shown in Figs. 5–7, respectively. The GB plane distributions for 15°, 25°, 35° and 45° misorientations about the [100] axis for the undoped and 0.3% Ca-doped MgO are illustrated in Fig. 5. For both samples, the GB plane distributions vary with misorientation angle. The maxima for the doped sample are approximately twice as high as in the undoped sample. This greater anisotropy is consistent with the GB plane distributions in the crystal reference frame. The tendency to terminate GBs on {100} planes means that the GB normals are usually either perpendicular to the misorientation axis or parallel to the misorientation axis. In the former case, these are pure tilt boundaries and are distributed along the vertical line joining [010] and [0$\bar{1}$0]. The endpoints of this line are labeled by open circles. In the latter case, they are pure twist boundaries and have either [100] or [$\bar{1}$00] orientations. These points are labeled by the solid circles. Undoped MgO shows a preference for pure tilt GBs at relatively low angles (15° and 25°), whereas {100} terminated twist boundaries are preferred at higher angles (35° and 45°). This tendency is also present, although less marked, in the case of Ca-doped MgO, where both pure tilt and twist GBs display high values of MRD at each misorientation angle. Families of planes other than {100} are also identified as having higher than random frequencies at relatively low misorientation angles (15° and 25°) in MgO and more clearly at all misorientation angles in Ca-doped MgO. These higher index planes are geometrically necessary complements to the {100} plane on one side of the interface. For example, if a bicrystal with a 25° misorientation about [100] has a [001] plane bounding one of the crystals, the adjoining plane in the second crystal must be misorientated along the [100] zone by 25° (see arrows in Fig. 5(a)). Thus, the multiple peaks along the [100] zone arise from complementary GB planes that make up asymmetric tilt boundaries (see also arrows in Fig. 5(b)).

The GB plane distributions for misorientations about the [110] axis are shown in Fig. 6. The distributions show maxima at the positions of {100} planes and their geometrically necessary complements. The ranges of anisotropy are similar, but in the undoped sample, the maxima are confined to the [110] zone of pure tilt boundaries, with the (001) plane matched with a geometrically necessary complement. In the doped sample, however, (001), (010) and (100) planes all display maxima. The influence of Ca on increasing the population of {100} planes is

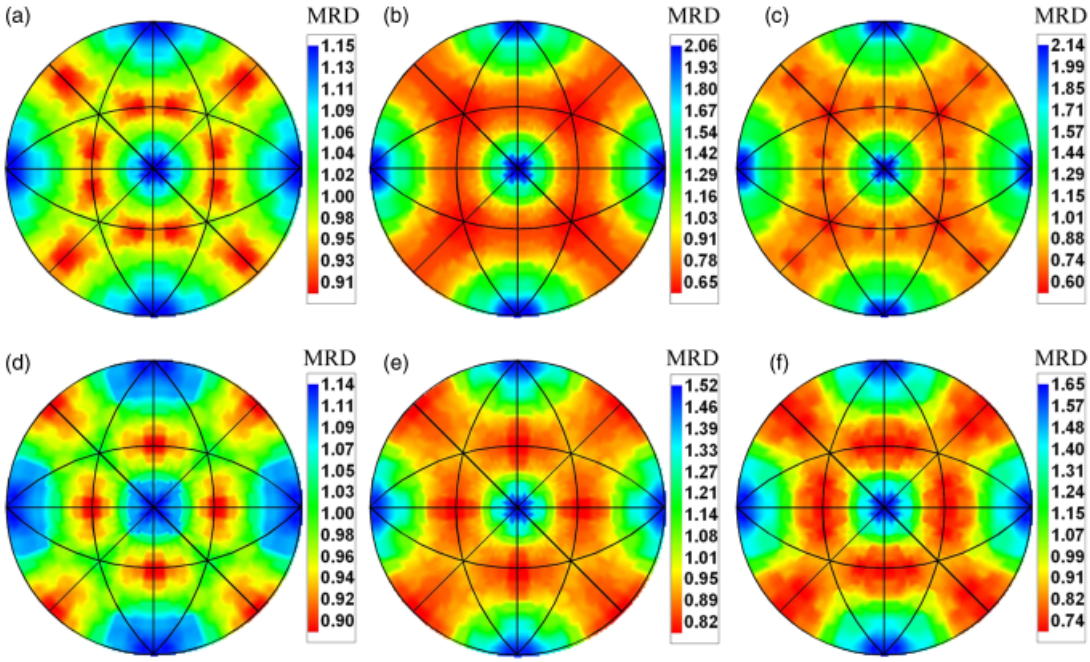

Fig. 4. Distribution of grain boundary plane orientations in the crystal reference frame, displayed as [001]-centered stereographic projections. The [100] direction is horizonal and to the right. Figures (a)–(f) show the raw data for (a) the undoped MgO, (b) 0.3% Ca-doped MgO, (c) 0.1% Ca-doped MgO, (d) Sr-doped MgO, (e) Ba-doped MgO, and (f) Y-doped MgO.

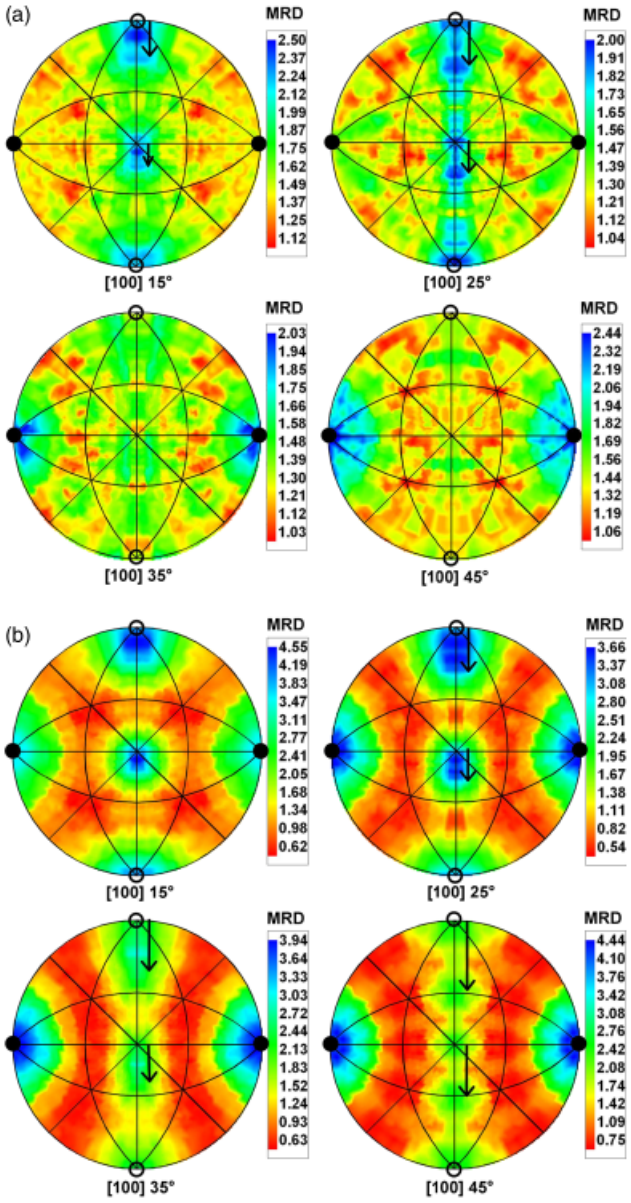

Fig. 5. Stereograms showing the distribution of grain boundary (GB) plane orientations in the bicrystal reference frame for specific GB misorientations (15°, 25°, 35°, and 45° about [100]) for (a) undoped MgO, and (b) 0.3% Ca-doped MgO. The [100] misorientation axis is horizontal and points to the right. Pure twist orientations occur along the horizontal line marked with filled circles, and pure tilt orientations occur along the vertical line connecting the open circles. Arrows indicate the position of the complementary crystal plane for any GB containing one {100} plane inclined by the misorientation angle along the tilt axis.

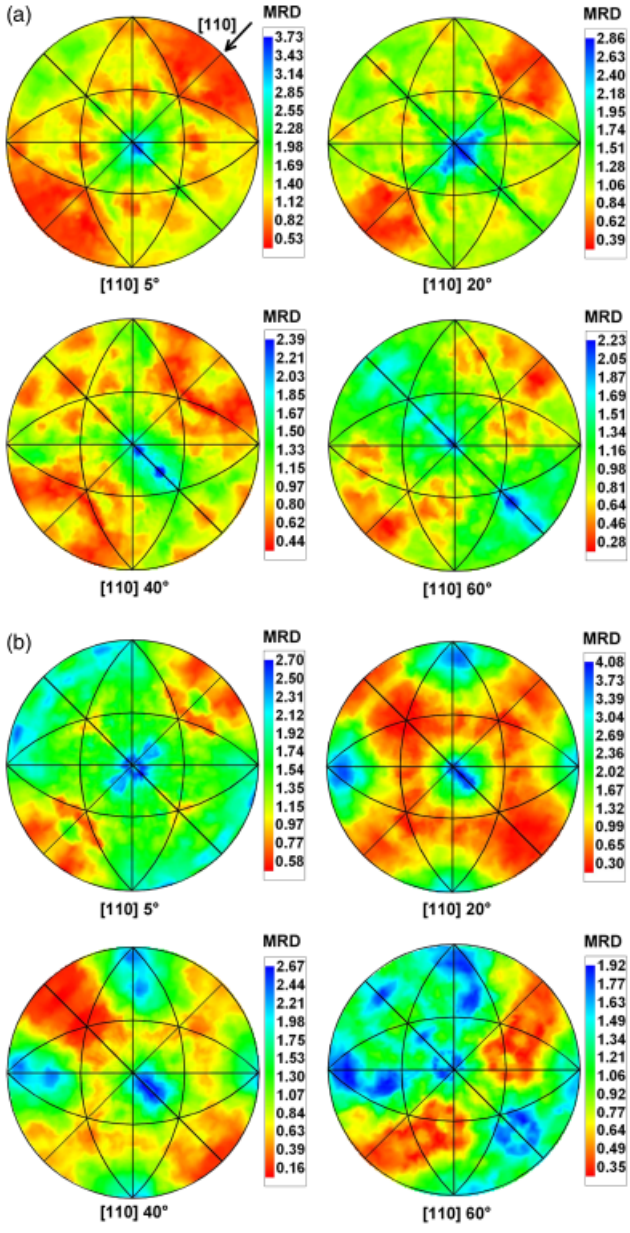

Fig. 6. Stereograms showing the distribution of grain boundary plane orientations in the bicrystal reference frame for specific grain boundary misorientations (5°, 20°, 40°, and 60° about [110]) for (a) undoped MgO and (b) 0.3% Ca-doped MgO. The orientation of the [110] misorientation axis is indicated by an arrow in (a).

demonstrated most clearly in the GB plane distributions for [111] type misorientations, shown in Fig. 7. For the undoped sample, Fig. 7(a), the maxima at 20°, 40°, and 60° are clearly located at (111), which corresponds to the orientation of the pure twist boundary. For the doped sample, Fig. 7(b), the maxima for 5°, 20°, and 30° misorientations occur at the orientations of {100} planes and their geometrically necessary complements. Only for the Σ3 boundary ([111] 60°) is the (111) GB plane favored; this is a twin boundary.

The GBCD measured stereologically in the present work is entirely consistent with the GBCD determined previously by serial sectioning.[13] Although it was not intentionally added, the previous sample had a small amount (~0.2%) of Ca.[17] The only significant differences between the results presented by Saylor *et al.*[13] and the present results occur at the (111) position; because of the (111) axial texture in the sample studied in the earlier work, (111) planes were, on average, oriented parallel to the sample surface. As a result, their frequency was not accurately measured. The present work therefore presents a more complete and accurate picture of the GBCD of Ca-doped MgO.

IV. Discussion

(1) Segregation Results

The results presented here demonstrate that the five parameter GBCD can be influenced by the addition of segregating impurities. It is therefore useful to begin with a discussion of the quantification of segregation effects. Observations of GB segregation of the dopants used in this study were reported in Section III.1 in the form of Auger peak ratios. Because the detection sensitivity in AES differs significantly from one element to another, these ratios cannot be used directly to compare how strongly the different dopants segregate to GBs. Although the

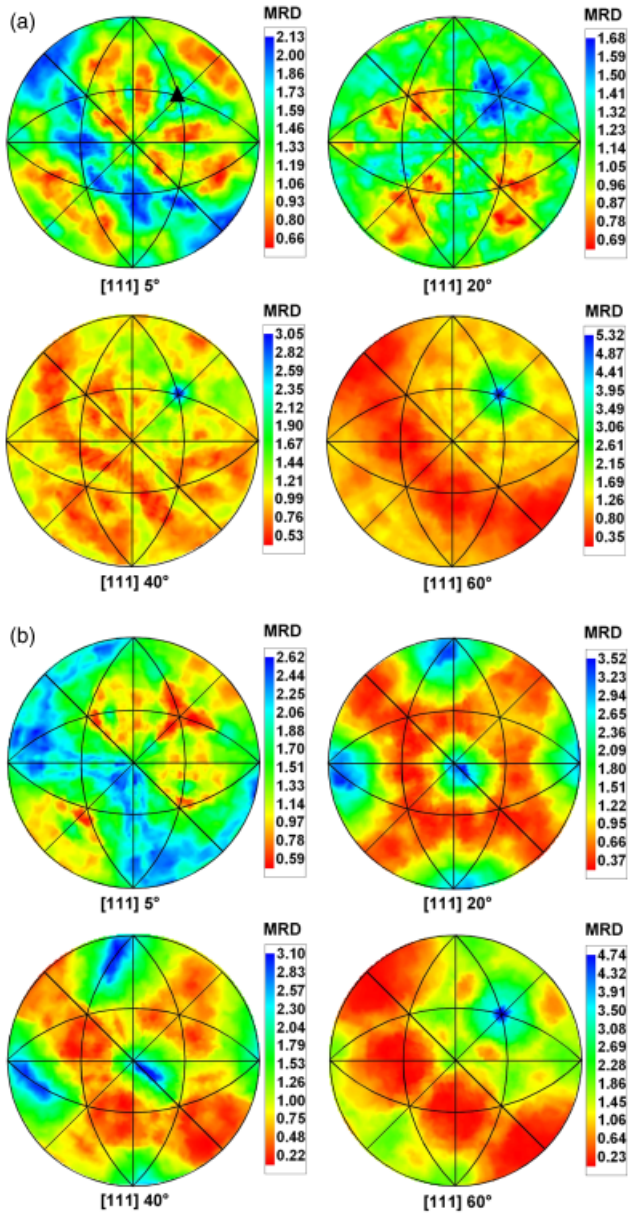

Fig. 7. Stereograms showing the distribution of grain boundary plane orientations in the bicrystal reference frame for specific grain boundary misorientations (5°, 20°, 40°, and 60° about [111]) for (a) undoped MgO and (b) 0.3% Ca-doped MgO. The orientation of the [111] misorientation axis is indicated by a triangle in (a).

Auger sensitivities of different elements are known when they are present in elemental form,[18] the relative sensitivities when they are present in the form of oxides can be quite different, and have not been studied systematically. As a rough guide, we give the relative elemental sensitivities of the materials mentioned in this study; Mg: Si: Ca: Sr: Y: Ba::1:4.8: 4.6: 0.6: 1.3: 1.1, which can be useful in understanding the results obtained. The average values of the Ca/Mg and Ba/Mg Auger peak ratios observed in Ca- and Ba-doped samples were 0.38 and 0.19, respectively. Because segregation is expected to increase with increasing difference between the solute and solvent ionic radii, one would expect stronger GB segregation of Ba than Ca (see Table I), other factors being equal. Given that the Auger sensitivity for Ba could be smaller than that of Ca by as much as a factor of four, this means that the Ba/Mg ratio would need to be multiplied by four to be quantitatively compared with the Ca/Mg ratio. Also, the lack of a measureable Sr signal from GBs in the Sr-doped sample may be connected with its very low Auger sensitivity, even though it is expected to segregate more strongly than Ca, on the basis of ionic radius differences.

In spite of the difficulty in determining absolute levels of segregation, the results reported in Section III.1 can be used effectively to assess the variability of GB segregation of a given dopant, i.e. the manner in which its segregation varies from one GB to another, or from one side of a given GB to the other. This variability arises because of the differences in crystallography, as was convincingly established previously in a study of Nb segregation to TiO_2 GBs, where both GB segregation levels and GB crystallography were determined.[6] Thus, the differences between Ca/Mg and Ba/Mg peak ratios shown in Fig. 2 for Ca-doped and Ba-doped samples, respectively, are interpreted as reflecting an anisotropy of segregation that stems from the differences in crystallographic structure from GB to GB, and from one side of a GB to the other. Such conclusions have been reached previously in the case of Ca-doped MgO[8] and Nb-doped TiO_2.[6]

(2) Segregation and GB Energy

Another issue that needs to be addressed is the relationship between the strength of segregation and the GB energy. In an analysis of the results of Nb segregation to TiO_2 GBs it was concluded that the higher the GB energy, the stronger the GB segregation of dopant.[19] While this conclusion was strongly supported by the results on Nb-doped TiO_2, it has since been determined from models of interfacial segregation that this trend is not necessarily general.[20] Depending on the magnitudes of the parameters that control segregation behavior, it is also possible for segregation to be strongest at the lowest energy interfaces or GBs, i.e. no simple universal relationship exists between the strength of interfacial segregation and interfacial energy. Furthermore, the models show that the energetic ordering of interfaces is generally modified by segregation.[20] More recent investigation with similar models has determined that size mismatch between solute and solvent is the most important factor in changing the energetic ordering of interfaces, and that the larger the solute misfit, the more significant the energetic reordering.[21]

(3) GB Energy Anisotropy in MgO and its Relation to the GBCD

There exists a relationship between GB energy and the surface energies associated with the crystallographic planes that bound the crystals adjoining the GB. This conclusion has emerged from the GB computer simulations of Wolf,[22] which showed that GB energy depends linearly on the mean energy of the two surfaces, although GB energy is not proportional to mean surface energy. In metal oxides, a similar concept was used by Saylor *et al.*[23] to express GB energy as

$$\gamma_{GB} = \gamma_{S1} + \gamma_{S2} - E_B$$

where γ_{GB} is the GB energy, γ_{S1} and γ_{S2} are the surface energies corresponding to the two adjacent GB planes, and E_B is an orientation-dependent binding energy which accounts for the bonding that occurs when two half-crystals are joined together to form the GB. From the measured anisotropy of both the surface and GB energy in MgO, it was concluded that for high angle GBs, to a first approximation, the term E_B is constant. Saylor *et al.*[23,24] also determined that both $\lambda(n)$ and $\lambda(\Delta g,n)$ are inversely correlated with GB energy, i.e. the lower the energy of a given GB the more frequently it appears in the microstructure. In particular, because the GB energy is lowest for GBs bounded by {100} planes, and highest for GBs bounded by {111} planes, the observed GB plane distribution in MgO showed a maximum at {100} and a minimum at {111}.

Because segregation lowers GB energy, and the level of GB segregation is anisotropic, it is generally expected that doping a material with interfacially active solute will modify the frequency with which GBs of different types appear. The results here suggest that in MgO, segregating impurities do not influ-

ence the grain orientation texture or the misorientation texture. For the undoped MgO, as well as Ca- and Ba-doped MgO specimens, the maximum frequency ranges from 1.1 to 1.4 MRD, i.e. the population of grains is practically equally distributed over the whole domain of crystal orientations. In the case of the Y-doped sample, we observe a slight ⟨111⟩ axial preference with a maximum frequency of 2.4 MRD. This could be a sampling artifact due the larger average grain size of the Y-doped sample (see Table II) and the smaller number of grains analyzed (see Table III).

(4) λ(n): Distribution of GB Planes in the Crystal Reference Frame

Figure 4 shows the effects of doping on the distribution of GB planes in MgO. The main difference between the distributions is the intensity of the peak at {100} and noting this, it becomes clear that Ca segregation at GBs plays a more significant role in changing the GB plane distribution of MgO than other dopants. This result is somewhat surprising, given that based on ionic size considerations, Sr and Ba would be expected to segregate more strongly to MgO GBs than Ca, and to have a larger effect on the energetic ordering of GBs.[21] This apparent inconsistency could be due to a lower solubility of Sr and Ba in MgO, such that at the nominal 0.1% doping level of these solutes, the limit of solubility is exceeded. Lower solubilities would mean lower respective bulk concentrations of these dopants in the MgO solid solutions, and hence lower GB concentrations. However, the bulk solubilities of Sr and Ba in MgO are not available in the literature, and the apparently higher effective concentration of Ba than Ca in MgO GBs observed by AES (see Section IV.1) makes this interpretation less likely. Finally, it is possible that because of its smaller ionic size, Ca is more easily accommodated at GBs that are comprised of at least one {100} terminating plane than at other GBs, whereas Sr and Ba may have higher misfit energies at all GBs, and may therefore be more evenly distributed among GBs of all orientations. Unfortunately, no simple models are available at this time to investigate such a hypothesis in MgO. Thus, the reasons for smaller effects of Sr and Ba on $\lambda(n)$ are unclear at this time.

(5) λ(Δg,n):GBCD of Undoped and 0.3% Ca-Doped MgO

Figures 5–7 provide additional details on the relative frequencies and stabilities of GB planes in undoped and Ca-doped MgO. The general trends in the measurements have been described above in Section III.5. The principal observation is that Ca is effective in stabilizing (and increasing the relative areas of) the {100} planes. As discussed above, the origin of this effect in comparison to Sr and Ba is not clear and it is therefore not useful to speculate on the role of segregation effects at specific misorientations.

(6) Overview

Solute segregation at interfaces (i.e., a positive excess interfacial solute concentration) decreases the interfacial energy, according to the Gibbs adsorption isotherm[1]:

$$d\gamma = -\sum_i \Gamma_i d\mu_i$$

where γ is the interfacial energy, and Γ_i and μ_i are the adsorption and chemical potential of the ith component, respectively. In order to determine the change in surface energy accompanying segregation (or adsorption), one therefore needs quantitative information on both the strength of the segregation and the variation of chemical potential. In the present study these quantities were unavailable. However, the measurements performed here do provide some indirect information on the anisotropy of GB energy of MgO, because it has been shown previously that the frequency at which GBs appear in MgO polycrystals is approximately inversely related to the GB energy distribution.[13] What is unequivocally shown by the results is that the frequency of appearance of GBs terminated on one side by specific crystal planes, in undoped MgO, is changed significantly by certain dopants, and that the segregation of the dopants is strongly anisotropic. (It should be recalled that the effects of Sr on the GB plane distribution is weak, and that segregation of Sr could not be confirmed). The results therefore demonstrate that the presence of dopants at the GBs modifies the GB energy distribution, i.e. GB energy anisotropy, as well as the energetic order of GB energy. These results are consistent with predictions of recent models of interfacial segregation.[20,21]

V. Summary

We have investigated the changes in the GB distribution that result from doping MgO with Ca, Sr, Ba, and Y. AES measurements were able to establish that Ca, Ba, and Y segregate to the GBs in MgO, but segregation of Sr could not be confirmed. Both the orientation and the misorientation distributions of MgO were unaffected by the presence of segregating dopants. In both pure and doped MgO, the GB plane distribution shows a preference for GBs that include at least one {100} terminating plane. This tendency is significantly increased by GB segregation of Ca, and to a lesser extent by Ba and Y segregation. Thus, segregation preferentially decreases the energy of the lowest energy {100} GBs of MgO. The current results illustrate the possibility of controlling the GBCD by judicious doping with suitable GB segregating impurities, and thereby open up new approaches for controlling the macroscopic properties of polycrystals that depend on the GBCD.

References

[1]J. W. Gibbs, *The Scientific Papers of J. Willard Gibbs*, Vol. 1, pp. 219–331. Dover, New York, NY, 1961.

[2]G. S. Rohrer, D. M. Saylor, B. S. El-Dasher, B. L. Adams, A. D. Rollett, and P. Wynblatt, "The Distribution of Internal Interfaces in Polycrystals," *Z. Metallkunde*, **95**, 197–214 (2004).

[3]A. Roshko and W. D. Kingery, "Segregation at Special Boundaries in MgO," *J. Am. Ceram. Soc.*, **68**, C331–3 (1985).

[4]S. M. Bruemmer, L. A. Charlot, J. S. Vetrano, and E. P. Simonen, "Radiation-Induced Grain Boundary Segregation in Austenitic Stainless Steels"; pp. 251–6 in *Materials Research Society Symposium Proceedings, Vol. 373, Microstructure of Irradiated Materials*, Edited by I. M. Robertson, L. E. Rehn, S. J. Zinkle, and W. J. Phythian. Materials Research Society, Pittsburgh, PA, 1995.

[5]M. Menyhard and C. J. McMahon Jr., "Anisotropic Distribution of the Segregated Atoms between the Two Fracture Surfaces," *Scr. Metall. Mater.*, **25**, 935–8 (1991).

[6]Y. Pang and P. Wynblatt, "Correlation between Grain Boundary Segregation and Grain Boundary Plane Orientation in Nb-Doped TiO_2," *J. Am. Ceram. Soc.*, **88**, 2286–91 (2005).

[7]Y. Pang and P. Wynblatt, "Effects of Nb Doping and Segregation on the Grain Boundary Plane Distribution in TiO_2," *J. Am. Ceram. Soc.*, **89**, 666–71 (2006).

[8]F. Papillon, P. Wynblatt, and G. S. Rohrer, "Segregation of Calcium to Magnesium Oxide Grain Boundaries"; in *Proceedings of the 2nd International Conference on Recrystallization and Grain Growth*, Edited by B. Bacroix, J. H. Driver, R. Le Gall, C. Maurice, R. Penelle, H. Réglé, and L. Tabourot. *Mater. Sci. Forum*, 469, 789–794 (2004).

[9]P. W. Tasker, E. A. Colburn, and W. C. Mackrodt, "Segregation of Isovalent Impurity Cations at the Surfaces of MgO and CaO," *J. Am. Ceram. Soc.*, **68**, 74–80 (1985).

[10]P. Wynblatt, G. S. Rohrer, and F. Papillon, "Grain Boundary Segregation in Oxide Ceramics," *J. Eur. Ceram. Soc.*, **23**, 2841–8 (2003).

[11]R. D. Shannon and C. T. Prewitt, "Effective Ionic Radii in Oxides and Fluorides," *Acta Cryst.*, **B25**, 925–46 (1969).

[12]R. D. Shannon, "Revised Effective Ionic Radii and Systematic Studies of Interatomic Distances in Halides and Chalcogenides," *Acta Cryst.*, **A32**, 751–67 (1976).

[13]D. M. Saylor, A. Morawiec, and G. S. Rohrer, "Distribution of Grain Boundaries in Magnesia as a Function of Five Macroscopic Parameters," *Acta Mater.*, **51**, 3663–74 (2003).

[14]D. M. Saylor, B. S. El-Dasher, B. L. Adams, and G. S. Rohrer, "Measuring the Five Parameter Grain Boundary Distribution from Observations of Planar Sections," *Metall. Mater. Trans.*, **35A**, 1981–9 (2004).

[15]S. I. Wright and R. J. Larsen, "Extracting Twins from Orientation Imaging Scan Data," *J. Microscopy*, **205**, 245–52 (2002).

[16]H. M. Miller and G. S. Rohrer, "Evolution of the Grain Boundary Character Distribution in Strontium Titanate with Grain Growth"; pp. 335–42 in *Ceramic Transactions, Vol. 201, Applications of Texture Analysis*, Edited by A. D. Rollett. American Ceramic Society, Westerville, OH, 2009.

[17]D. M. Saylor, D. E. Mason, and G. S. Rohrer, "Experimental Method for Determining Surface Energy Anisotropy and its Application to Magnesia," *J. Am. Ceram. Soc*., **83**, 1226–32 (2000).
[18]L. E. Davis, N. C. MacDonald, P. W. Palmberg, G. E. Riach, and R. E. Weber, *Handbook of Auger Electron Spectroscopy*, 2nd edition, Perkin Elmer Corporation, Eden Prairie, MN, 1978.
[19]P. Wynblatt, Z. Shi, Y. Pang, and D. Chatain, "On the Relation Between the Anisotropies of Grain-Boundary Segregation and Grain-Boundary Energy," *Z. Metallkunde*, **96**, 1142–6 (2005).
[20]P. Wynblatt and D. Chatain, "Anisotropy of Segregation at Grain-Boundaries and Surfaces," *Metall. Mater. Trans*., **37A**, 2595–620 (2006).
[21]P. Wynblatt and D. Chatain, "Surface Segregation Anisotropy and the Equilibrium Shape of Alloy Crystals," *Rev. Adv. Mater. Sci*., **21**, (2009), in press.
[22]D. Wolf, "Structure-Energy Correlation for Grain-Boundaries in fcc Metals—IV Asymmetrical Twist (General) Boundaries," *Acta Metall. Mater*., **38**, 791–8 (1990).
[23]D. M. Saylor, A. Morawiec, and G. S. Rohrer, "The Relative Free Energies of Grain boundaries in Magnesia as a Function of Five Macroscopic Parameters," *Acta Mater*., **51**, 3675–86 (2003).
[24]D. M. Saylor, A. Morawiec, B. L. Adams, and G. S. Rohrer, "Misorientation Dependence of the Grain Boundary Energy in Magnesia," *Interface Sci*., **8**, 131–40 (2000). □